Martínez Ramos, C.; Lebourg, M. (2015). Three-dimensional constructs using hyaluronan cell carrier as a tool for the study of cancer stem cells. Journal of Biomedical Materials Research Part B: Applied Biomaterials. 103(6):1249-1257. doi:10.1002/jbm.b.33304.

Three-dimensional constructs using hyaluronan cell carrier as a tool for the study of cancer stem cells

Cristina Martínez-Ramos,[1] Myriam Lebourg[1,2]

[1]Center for Biomaterials and Tissue Engineering, Universitat Politécnica de Valencia, Camino de Vera s/n, 46022 Valencia, Spain
[2]Networking Research Centre on Bioengineering, Biomaterials and Nanomedicine (CIBER-BBN), Valencia, Spain

Received 14 May 2014; revised 4 September 2014; accepted 1 October 2014
Published online 00 Month 2014 in Wiley Online Library (wileyonlinelibrary.com). DOI: 10.1002/jbm.b.33304

Abstract: Background: Cancer research focuses increasingly on cancer stem cell study as those cells are thought to be the root of chemo and radioresistance of the most aggressive cancer types. Nevertheless, two-dimensional (2D) cell culture and even three-dimensional (3D) spheroid models, with their limited ability to reflect cell-extracellular matrix interactions, are not ideal for the study of cancer stem cells (CSCs). In this study, we establish a 3D *in vitro* cancer model using a synthetic and natural scaffold with tunable features and show that U87 cells cultured in this system acquire a stem-cell like phenotype. Methods: U87 astrocytoma cells were grown on polycaprolactone (PCL)−2D flat substrates (2D) and PCL-3D scaffolds (3D) eventually containing hyaluronic acid (3D-HA). Cell viability, growth patterns, morphology, and cell surface marker expression (CD44, RHAMM and CD133) were studied to assess the effect of 3D culture and presence of HA. Results: 3D scaffold, but most prominently presence of HA induced changes in cell morphology and marker expression; 3D-HA cultures showed features of aggregates; moreover, markedly increased expression of Nestin, CD44, RHAMM, and CD133 in 3D-HA scaffolds were found. Conclusions: the behavior of U87 in our 3D-HA model is more similar to tumor growth *in vivo* and a stem-like phenotype is promoted. Thus, the 3D-HA scaffold could provide a useful model for CSCs study and anti-cancer therapeutics research *in vitro* and may have preclinical application for the screening of drug candidates. J Biomed Mater Res Part B: Appl Biomater 00B: 000–000, 2014.

Key Words: 3D scaffold, hyaluronic acid/hyaluronan, cancer stem cells, hydrogel, tumor model

How to cite this article: Martínez-Ramos C, Lebourg, M. 2014. Three-dimensional constructs using hyaluronan cell carrier as a tool for the study of cancer stem cells. J Biomed Mater Res Part B 2014:00B:000–000.

INTRODUCTION

Glioblastoma is one of the most lethal cancer types, and its high malignancy leads to a median survival of only 12 months.[1] Glioblastoma cells show resistance to radiotherapy and chemotherapy, and this resistance is mainly thought to be due to a subpopulation of highly resistant cancer stem cells (CSCs).[2,3] Such cells share many characteristics of stem cells such as self-renewal capacity, undifferentiated state, multipotential differentiation ability[4]; presence of cells with increasingly undifferentiated state correlates with poor prognosis of glioblastoma patients.[5] In glioma, the presence of neural progenitors expressing genes characteristic of neural stem cells such as CD133, Sox2, musashi-1, bmi-1, able to form neural spheres, has been described and is increasingly studied due to its clinical relevance in glioma treatment.[6–8] Thus, to develop successful strategies to treat gliomas, it seems desirable to work with populations enriched in CSCs as a worst-case scenario. Nevertheless, standard culture conditions using two-dimensional (2D) substrates and serum-containing medium do not favor the expression of a CSC phenotype,[9] and most works studying glioma CSCs use serum-free media supplemented with costly growth factors to induce CSC phenotype and obtain CSC-rich populations from clinical specimens[10] or standard cell lines.[11]

Generally, traditional 2D models are very limited and lead to poor predictability of *in vitro* assays, which is no surprise, as molecular targets are modulated by the microenvironment including cell-cell, cell-stroma, and cell-matrix interaction, as well as other mechanisms related to the tumor microarchitecture (central hypoxia and lack of nutrients), all lacking in a 2D petri dish. These differences in the microenvironment cause changes in cytoskeletal organization, extracellular matrix production, proliferation, or cell membrane receptor expression to cite only a few.[12,13] For that reason in the last 10 years three-dimensional (3D) models of growing using scaffolds complexity have been developed in order to mimic

Additional Supporting Information may be found in the online version of this article.
Correspondence to: C. Martínez-Ramos; e-mail: cris_mr_1980@hotmail.com
Contract grant sponsor: Spanish Generalitat Valenciana (project GV/2012/026)
Contract grant sponsors: National R&D&i Plan (2008–2011; CIBER-BBN), Iniciativa Ingenio 2010, Consolider Program, CIBER Actions, and Instituto de Salud Carlos III (European Regional Development Fund)

more closely the tumor microenvironment,[14–16] working with multicellular aggregates or spheroids[17] or with extracellular matrix (ECM) based hydrogels Matrigel-like,[18–20] which have led to valuable forthcomings in the knowledge of pathological mechanisms. Nevertheless those models present some problems due to the absence of cell-matrix interaction in the case of spheroids such interaction is said to be determinant in the cell response, especially to drugs[13] and in the case of using animal tissue derived matrix, there may be substantial variations of composition between batches which affect the reproducibility of assays and comparative studies.[21] For this reason, recent work has been dedicated to engineer tumorous constructs using synthetic porous materials such as poly (L-lactic acid),[22] poly(lactide-*co*-glycolide),[23] or hydrogels which production mode is more standardized and batch-to-batch variability is more limited, as chitosan,[24] collagen,[25–27]or hyaluronic acid (HA).[28] This kind of model showed to be more relevant physiologically[29] reproducing tumor-like characteristics as internal hypoxia,[30] metabolic activity, or paracrine secretion.[24] Cells grown on 3D substrates have shown high tumorigenicity when implanted in animals when compared with 2D cultured cells.[31] Most importantly, cell survival upon treatment with standard antitumoral drugs such as doxorubicin, paclitaxel or tamoxifen was significantly higher in 3D constructs.[22,24] Up to date, there is no significant data studying the differentiation state of 3D cultured tumoral cells or the influence of 3D culture on CSCs subpopulations.

HA is present in high amounts in the tumor stroma, and cancer is often accompanied by alterations of HA metabolism.[32] These alterations use to be related with a high grade of malignancy and metastasis.[32–34] HA interplays in several tumorigenic mechanisms either directly (angiogenic effect of oligomers of HA) or indirectly due to cancer cell interaction mediated by membrane receptors CD44 and RHAMM. Cancer cell interaction with extracellular matrix polysaccharide hyaluronan (HA), mostly mediated by membrane receptors CD44 and RHAMM, induces a more aggressive and invasive phenotype,[35,36] but to date there have been no reports of its influence on differentiation status of glioma cells. Here, we wanted to investigate the hypothesis that 3D culture in presence of hyaluronan induces a more undifferentiated phenotype, which would prove useful for the study of glioma CSCs and the development of therapies against glioma.

In this work, we use 3D materials consisting of a HA cell carrier phase within synthetic polycaprolactone (PCL) scaffolds previously developed in our laboratory and study the behavior of U87 glioma cells in presence of HA (3D-HA), comparing their behavior with standard 3D culture in a PCL scaffold (3D) or 2D culture on PCL plane samples (2D) to assess their effect on differentiation state of U87 and their suitability as 3D model cultures for drug discovery.

MATERIALS AND METHODS

Preparation of scaffolds and plane samples

Scaffolds were prepared by a mixed particle leaching/freeze extraction process, as described previously.[37] Acrylic microspheres (Lucite International, mean diameter 200 μ) were used as a porogen. Polycaprolactone (PCL, Mn∼50 kDa, Polysciences) was dissolved at 20% (w/w) in dioxane and mixed with the porogen in Teflon molds. Molds were immersed in liquid nitrogen and frozen. Dioxane was removed by freeze-extraction during 3 days at −20°C in ethanol. Then, porogen was leached in ethanol at 40°C during one week. Cylindrical samples of 5 mm diameter were stamped out of the disks and height was homogenized to 3 mm.

For 2D controls, PCL was dissolved in chloroform (10% w/v) and cast over Petri dishes. Solvent was allowed to evaporate for 1 day and round disks of 8 mm diameter were stamped out of the obtained films. All samples (plane samples and scaffolds) were dried to constant weight and irradiated with γ-ray irradiation at 25 kGy before use for cell culture.

Modification of hyaluronan

Hyaluronan (from Streptococcus Equi, Sigma-Aldrich, Mn∼1.5 to 1.8 × 10^6 Da) was chemically modified in order to allow for cell encapsulation following the protocol by Darr and Calabro.[38] Shortly, hyaluronan was dissolved in MES buffer (250 m*M*) containing NaCl (150 m*M*) and NaOH (75 m*M*) at pH 5.75. After complete dissolution, modification of hydroxyl moieties with tyramine using carbodiimide chemistry was carried out by mixing 2:1 molar ratio of tyramine hydrochloride (Sigma-Aldrich, Spain) to hydroxyl moieties of hyaluronan, 1-ethyl-3-(3-dimethylaminopropyl) carbodiimide (EDAC, 1:1 to tyramine; Sigma-Aldrich, Spain) and *N*-hydroxysuccinimide (NHS, 1:10 to EDC; Sigma-Aldrich, Spain). Reaction was carried out during 24h at 37°C in water bath. Then obtained tyramine-substituted hyaluronan (TS-HA) was dialyzed, first against 150 m*M* NaCl, and then against ultrapure water. When used for cell culture, TS-HA was first filtered at 0.2 um for sterilization and lyophilized in a sterile vial. When used for material characterization, TS-HA was directly lyophilized and was stored in a dry vessel at −20°C until experiments were performed. Substitution grade reached evaluated through measurement of spectrophotometric absorption at 470 nm[38] in NaCl 150 m*M* and comparison with a calibration curve of free tyramine at the same wavelength.

Cell culture

U87 glioma cell line from ATCC was a generous gift of J. Blanco, ICCC, Barcelona. Cells were cultured in standard conditions using high glucose DMEM (Sigma-Aldrich, Spain) supplemented with 1% glutamine, 1% P/S and 10% fetal bovine serum (FBS, Gibco). All cultures were maintained in a humidified incubator at 37°C, 5% CO_2, and 100% humidity. After expansion, the cells were detached for the cell-seeding experiments on scaffolds and plane samples.

Construct seeding and culture

PCL scaffolds were prehydrated overnight before seeding either in DMEM with FBS (for PCL pure scaffolds, thereafter described as 3D) or in phosphate buffer saline (PBS, for the PCL samples containing TS-HA, thereafter described as

3D-HA). Two-dimensional plane samples were also incubated with serum containing medium in order to favor protein adsorption on the surface and therefore cell adhesion onto them.

Cells were trypsinized from the cell culture flasks using trypsin-EDTA, and blocked using FBS. After centrifugation at 1000 rpm and counting, cells were resuspended in PBS with 2 g/L glucose (PBS-G) at high density for seeding. Scaffolds were seeded at a density of 400,000 cells/scaffold, whereas 2D was seeded at 50,000 cells/sample (this was calculated to have an equivalent cell density per surface). Three-dimensional was seeded using a volume of 30 μL/scaffold using a micropipette. For 3D-HA samples, first the concentrated (2x) cell suspension was mixed with an equal concentration of TS-HA solution in PBS-G to which 1:100 horseradish peroxidase (HRP 100 units/mL, Sigma-Aldrich) was added (TS-HA concentration had been previously calculated so as to have the nominal concentration after dilution with HRP and cells). Three-dimensional HA was seeded using a 250 μL syringe, injecting 30 μL of TS-HA/HRP/cells mix in each scaffold. Each scaffold was deposited in a U-bottom P96 well and 20 μL of hydrogen peroxide at 0.01% (Sigma Aldrich) was added. Two-dimensional samples were seeded at 0.5ml/well using a diluted cell suspension. Cells were allowed to adhere and TS-HA was allowed to crosslink for 1 hr, afterwards constructs were transferred on nonadherent 24-wells and covered with 750 μL DMEM supplemented with FBS. Half of the total volume of culture media was exchanged by fresh every 2 days. Constructs were cultured up to 7, 14, or 21 days and analyzed as described subsequently.

Electron scanning microscopy

Cryo-SEM was used in order to observe the internal morphology of TS-HA modified scaffolds (3D-HA, $n = 2$) in wet state. For Cryo-SEM, wet samples were carefully wiped with filter paper, mounted in a clamp, ultrafrozen, and then cryofractured; the sublimation temperature used was -60°C. Finally, samples were gold sputtered in the same cold vacuum chamber of a JEOL JSM6300 electron microscope and observed at an acceleration tension of 10 kV.

For observation of cell containing constructs, samples were fixed at the end of culture time with 2.5% glutaraldehyde and dehydrated in a series of increasingly concentrated ethanol. Samples were finally dried from hexamethyldisilazane, sputtered with gold and observed in a Hitachi S8400 electron microscope at an acceleration tension of 10 kV.

Hyaluronan content

The amount of crosslinked HA present in the scaffolds was determined using a thermogravimetric analyzer (TGA) from TA Instruments; samples were placed in a platinum pan and subjected to a heating scan from 50 to 800°C at 20°C/min under nitrogen atmosphere. The mass was monitored as a function of the temperature; results were analyzed using the software TA Analyzer from the instrument. Degradation peaks of HA and PCL were determined using bare crosslinked HA and PCL samples: using differential weight loss signal, onset and offset temperatures of the first degradation peak associated to HA at $T = 255^{\circ}$C were determined. From the weight scan of pure HA, it has been determined that the weight loss at this temperature corresponds to 35% of the total mass of HA. Weight loss percentage between these temperatures was determined, and corresponding HA weight in the sample was calculated.

Immunofluorescence imaging

At the end of culture time, three samples per group were rinsed with 0.1*M* PBS, pH 7.4, and fixed for 15 min in 4% paraformaldehyde (Panreac) at room temperature. Thereafter they were cryoprotected by immersion in 0.1*M* PBS containing 30% sucrose and included in OCT. Hundred micrometer thick sections were obtained by using a cryotome (Microm, HM 520) and washed with PBS. Samples were washed with PBS and treated with 0.1*M* glycine for autofluorescence quenching, and permeabilized using 0.5% Triton X100 (Sigma) in HEPES buffer 20 m*M* (Sigma Aldrich) supplemented with sucrose (Panreac, 10.3%), sodium chloride (Sigma Aldrich, 0.292%), and magnesium chloride (Scharlab, 0.06%). Blocking of unspecific sites was realized with PBS supplemented with 1% bovine serum albumin (BSA) for 1 h. Samples were then incubated with primary antibodies overnight at room temperature. Antibodies used were mouse anti Nestin (1:400, Abcam) with rabbit anti-Glial fibrillary acidic protein (GFAP, 1:400, DakoCytomation), or mouse anti-Vimentin (1:200, Sigma) with rabbit anti-CD44 (1:100, Abcam). Samples were washed with PBS containing 0.5% Tween 20 (Sigma-Aldrich) twice and incubated for 1 h with secondary antibodies (Alexa Goat anti Mouse 647 or Alexa Goat anti Rabbit 488, 1:400) at room temperature. Then, after washing with PBS containing 0.5% Tween 20, samples were stained with DAPI (1:5000, Sigma-Aldrich), washed with PBS and mounted using home-made Mowiol (Calbiochem) based mounting medium. Cells were observed in a Nikon Eclipse 80i fluorescence microscope or alternatively in an Olympus FV1000 confocal microscope.

Cell viability assay

Cell viability was measured using a metabolic assay using (3-(4,5-dimethylthiazol-2-yl)−5-(3-carboxymethoxyphenyl)−2-(4-sulfophenyl)−2H-tetrazolium) (MTS, Promega) assay. Samples at 1, 7, 14, and 21 days were washed using PBS, and MTS reagent mixed with phenol red free medium (1:5 v/v) was added. Samples ($n = 4$ at each time point in culture) were incubated in the dark during 1h at 37°C to allow reduction of MTS to formazan due to metabolic activity. Then aliquots were transferred to new wells and absorbance at 490 nm was read using a Victor 3 multiplate reader. Blank absorbances using unseeded materials were also read and subtracted to obtained absorbances.

Cytometry analysis

Cytometric analysis of cell surface markers CD44, RHAMM and CD133 was realized using a FC500 Cytomics cytometer

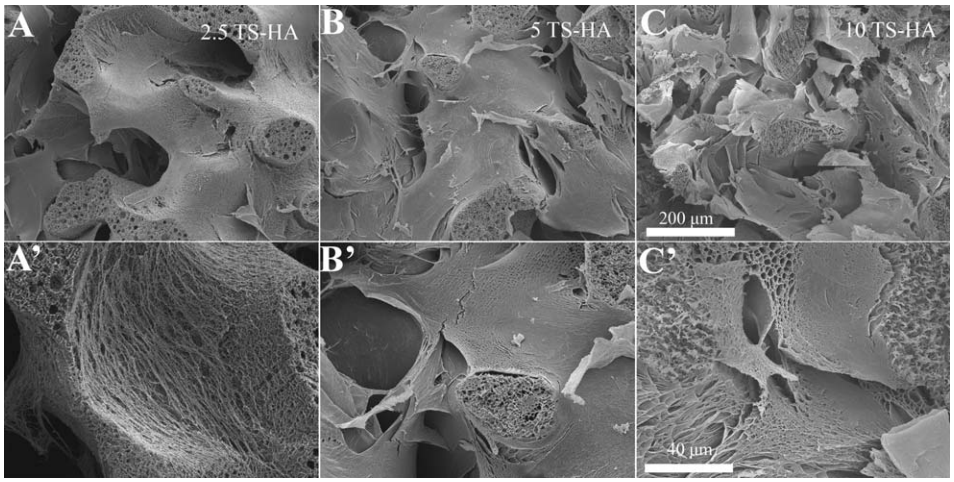

FIGURE 1. Cryo-SEM micrographs of porous architecture of PCL scaffolds at different concentrations of the HA: 2.5 mg/mL (A, A′), 5 mg/mL (B, B′) and 10 mg/mL (C, C′). Volume occupied by the hyaluronan gel increases at higher concentrations as observed on the micrographs. Scale bars: 200 μm (A–C) and 40 μm (A′–C′).

from Beckman Coulter. Cells were detached from the materials using mild enzymatic digestion with Accutase (Stempro), and approximately 2×10^5 cells were incubated with antibodies (CD44 (EPR1013Y epitope, Abcam, dilution 1:50) and RHAMM (2D6 epitope, Abcam, dilution 1:50) in phosphate buffered saline with 1% BSA) for 30 min at 4°C, washed extensively with PBS, marked with secondary antibodies (Alexa 647 and 488) for 30' and washed with PBS. For CD133, approximately 2×10^5 cells were incubated with PE-CD133 antibody (Milteny Biotech, 1:30). Cells were passed through the cytometer; secondary antibodies alone or PE-IgG were used as epitope controls. Gating values were determined using control cells grown on tissue grade TCPS in the same conditions. At least 10,000 cells were counted for each experiment ($n = 6$ samples), and experiments were conducted in triplicate.

Statistical analysis

Homogeneity of the variances was tested using a Levene Test in SPSS software. In case of homogeneity, analyses were performed using an ANOVA test. In case of in homogenous variances, a Kruskal Wallis test was used. For significant tests, a *post hoc* Tuckey test was used. Significance level was set at $p < 0.05$. The data collected are reported as the mean ± standard deviation.

RESULTS

Material characterization

The PCL scaffolds present the typical structure obtained by this technique, with a double porosity, macroporosity related with the porogen leaching and microporosity due to the phase separation and subsequent freeze extraction (Supporting Information Figure S1). TS-Hyaluronan had a substitution grade of 3% as determined using UV absorbance at 275 nm.[38] When TS-hyaluronan was mixed with peroxidase and injected inside of the pores in presence of hydroxide peroxide, it was efficiently crosslinked and insolubilized within the porous structure, as observed by Cryo-SEM (Figure 1). Using increasing concentrations of the TS-HA solution (2.5, 5, and 10 mg/mL), more space was occupied by the hydrogel phase.

Correspondingly, when determined quantitatively by TGA, the HA content showed to increase when using increasingly concentrated solutions for crosslinking (Figure 2). Thus, content and consistency of the hydrogel phase in the scaffolds can be easily tuned by varying the concentration of hyaluronan solution.

Cell culture

Cell seeding was optimized using different concentration of hyaluronan, and efficiency was seen to be similar at all concentrations tested as shown by metabolic test at 2 h post-seeding (Supporting Information Figure S2). MTS absorbance on 3D-HA was slightly lower than in 3D controls, but still good efficiency was obtained. Nevertheless, at longer times there was a slight drop in absorbance values that may be due to the leaching of cells at lower concentrations, which we related with the low viscosity of the gel or the possibility of some gel degradation during culture, and

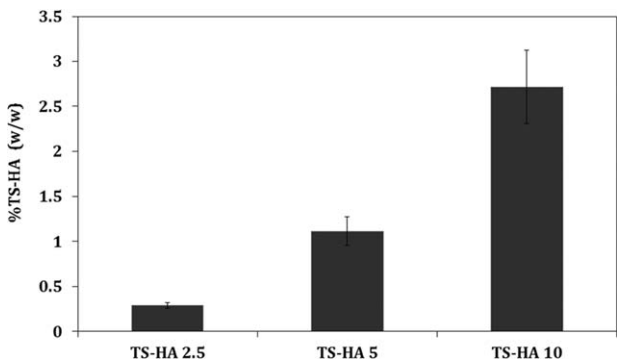

FIGURE 2. Dry content of TS-HA in the 3D-HA constructs with different concentrations of TS-HA (2.5, 5, and 10 mg/mL).

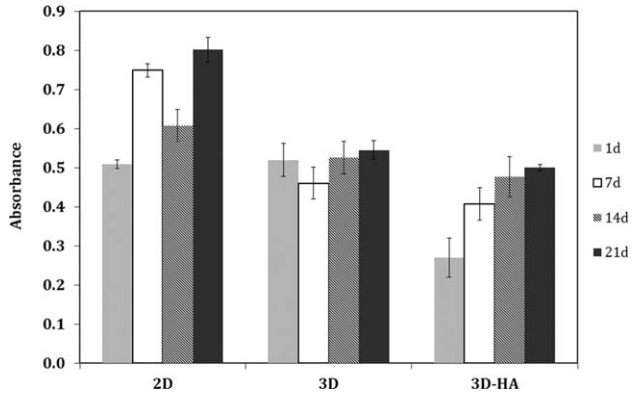

FIGURE 3. MTS metabolic assay at different times of culture *in vitro* (1, 7, 14, and 21 days) showing a slight increase in absorbance at large culture times.

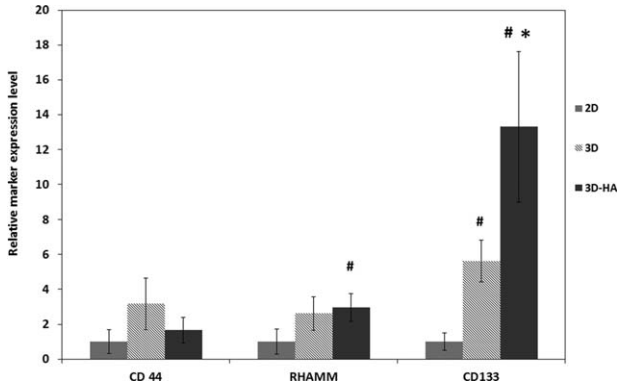

FIGURE 5. Evaluation of surface RHAMM, CD44 and CD133 expression in U87 using flow cytometry after 21 days of culture in 2D, 3D, and 3D-HA. Significant increase ($p < 0.05$) with respect to 2D are shown with # and to 3D with *.

so for further experiments, a concentration of 10 mg/mL TS-HA was used in the 3D-HA samples.

Cells were cultivated up to 3 weeks showing sustained metabolism during the culture time (Figure 3); nevertheless, MTS results did not show an exponential increase in metabolic rate as observed in other works.[39] Rather the absorbance remained stable over the weeks of culture, or increased slightly. Possible reasons for this result will be discussed later. We later checked viability using a live dead staining kit, and observed that nearly all cells remained viable after 14 days either in 2D [Supporting Information Figure S3(A)] or in the 3D construct [Supporting Information Figure S3(B)].

The cell morphology was observed by scanning electron microscopy (Figure 4): on 2D substrates [Figure 4(A)], cells show a either spread or spindle-like shape and are randomly distributed on the materials; when reaching confluence they tend to form aggregates. On 3D scaffolds [Figure 4(B)], cells spread also until covering the whole internal surface of the pore and then also form locally aggregates. In 3D-HA samples [Figure 4(C)], cells show a round morphology and are more prone to aggregate as clusters.

Cell phenotype in the different culture modes

On 3D culture, expression of cell-surface glycoprotein CD44 was slightly upregulated (Figure 5); this cell surface marker was also upregulated when cultured in hyaluronan-modified 3D structures (3D-HA), although in none of the conditions (3D or 3D-HA) differences were found to be statistically significant. Expression of RHAMM was also upregulated when cultivating in 3D, and further increased when cultivating in hyaluronan hydrogels (significant difference with respect to 2D control). At least, expression of CD133 was increased moderately on 3D culture (significant with respect to 2D) and dramatically when cultivating in 3D in presence of hyaluronan (3D-HA), showing statistically significant difference ($p < 0.05$) with respect to both 2D and 3D controls.

Cells were stained for Nestin, GFAP, Vimentin and CD44, in order to observe possible modulation of the expressed proteins due to culture mode and possible heterogeneities in the same sample. Results are shown in Figure 6: 2D samples showed staining for GFAP and CD44, whereas poor staining for Vimentin or Nestin was observed. In 3D, the staining for GFAP was more diffuse and cells lacked the fibrillar protrusions seen in 2D; this was more pronounced for 3D-HA samples; staining for Nestin was nearly absent in 2D, but increased in 3D and in 3D-HA; interestingly, increasing intranuclear localization of nestin staining was observed consistent with findings of others.[40,41] On the other hand, staining for Vimentin was not observed for all cells in 3D and 3D-HA culture, consistent with increasing phenotype heterogeneity in such cultures. Staining for CD44 was seen sporadically in all cultures and seemed to be more prominent in zones of increased cell–cell contact.

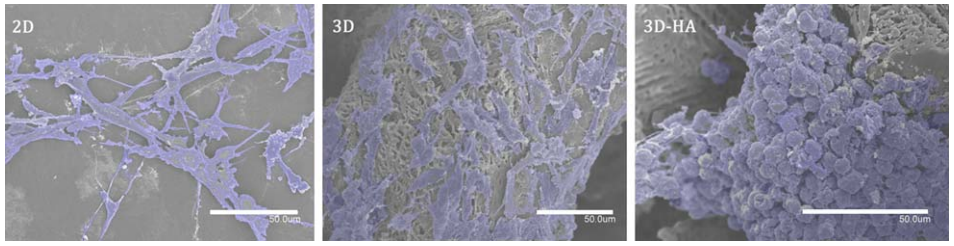

FIGURE 4. Cell morphology as observed by scanning electron microscopy after 21 days; for an easier observation of the adhesion and morphology in each substrate, cells were colored blue using Adobe Photoshop: on 2D (A) cells were randomly distributed and exhibited a spindle-like shape; on 3D (B) and 3D-HA (C) cells were formed aggregates and clusters. Scale bar: 50 μm. [Color figure can be viewed in the online issue, which is available at wileyonlinelibrary.com.]

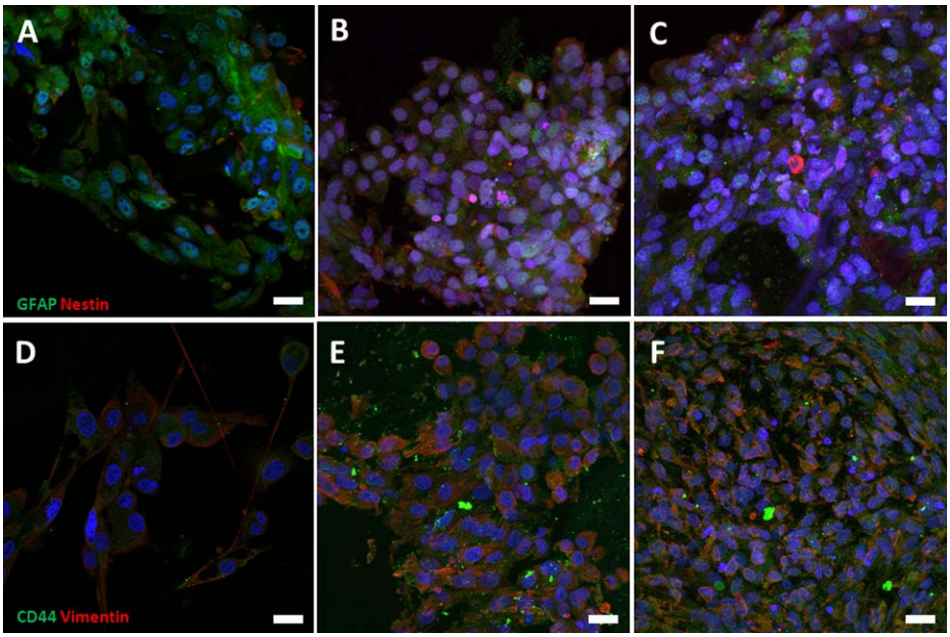

FIGURE 6. Double immunofluorescence staining showed expression of GFAP, Nestin (A–C) markers and CD44, Vimentin (D-F) in U87 cells. A, D: U87 cells on 2D; B, E: U87 cells on 3D; C,F: U87 cells on 3D-HA (Scale bar: 20 μm). [Color figure can be viewed in the online issue, which is available at wileyonlinelibrary.com.]

DISCUSSION

Numerous 3D cell culture models for cancer research are currently under focus due to the limitations related with traditional 2D cell culture models.[15] Cell behavior is known to be regulated by environmental factors, and 3D behavior often varies when compared with 2D behavior in terms of cytoskeletal development, cell marker expression, differentiation, and so forth.[12] Although various works have studied the influence of 3D culture on glioma cells morphology, proliferation, and response to cytostatic agents,[25,42] little is known about its influence on the differentiation state of glioma cells, while high recurrence rate of glioblastoma has been linked to the presence of subpopulations of CSCs. Moreover, most works studying CSCs work use the spheroid model[6,10] that does not reproduce the cell-matrix interaction component of cell response. In this work, we explore the influence of 3D culture and presence of HA on the differentiation state of U87 glioblastoma cell line.

PCL is widely used in bioengineering and tissue engineering due to its biocompatibility and stability. PCL scaffolds (Supporting Information Figure S1) produced in our lab show an interconnected pore structure and allow sustained growth of different cell types.[43,44] Besides, TS-modified hyaluronan allows encapsulation of live cells in an ECM-like microenvironment without significant loss of viability, and also shows *in vitro* stability over several weeks, being thus suitable for *in vitro* drug testing. Use of PCL together with HA gel permits a better manipulation, as PCL is much more rigid while HA is a very soft gel. U87 glioblastoma cells were found to proliferate and form neurosphere-like structures in 2D and 3D when reaching locally confluency. Whereas such neurospheres were easily leached out of 2D cultures during medium changes, they could sustain a consistent growth when sheltered by PCL 3D scaffold (3D) and HA gel phase (3D-HA). Cell density in the 3D constructs at large culture times were huge and similar to a tumor microenvironment as observable from the confocal pictures. Nevertheless, conversion of MTS into formazan was higher in 2D control than in 3D samples in our study. Similar results were obtained by Kievit et al.[25] *in vitro*, which they explained by a decreased mass transfer in 3D models as well as central hypoxia in the constructs which leads to decreased proliferation rates in absence of a vascular network. In contrast to 2D cultures which have easy access to nutrients and oxygen supplied by the culture medium, in 3D cultures, solutes must diffuse through the scaffold network before becoming available to cells.

It is reported in literature that differences in basal metabolism between 2D and 3D culture, as well as different diffusion rate of MTS containing medium in dense 3D culture also represents a limiting factor when studying cell proliferation in 3D.[45] This can be seen in Figure 3 at first day, where 2D and 3D samples show similar absorbances values although 3D samples were seeded at much higher density than 2D samples; absorbance in 3D-HA was still lower, whereas the constructs were seeded at the same density as 3D constructs. We observed that there is a significant adsorption of formazan compound onto the PCL scaffolds, which cannot be accounted for using the blank value of the curve (as in the blank value no transformation of MTS into formazan occurs). We measured using control culture wells and culture wells where a nonseeded PCL scaffold was added, that absorbance of MTS at similar cell density was decreased by 0.2 in the presence of a void scaffold due to

unspecific adsorption of formazan compound onto the scaffold (unpublished data). Thus, values can only be compared with respect to the same culture condition at different time and cannot be directly related to the cell number. Some studies suggest that other methods, such as XTT assay, could be more convenient when studying the proliferation of cells embedded in dense 3D matrices.[46] Here, another shortcoming is the leaching of cells during medium changes (which was unavoidable although medium change was realized changing 50% of medium each time), due to the tendency of U87 to form spheroids and detach from the materials, which can also explain that cell number does not increase steadily at large culture times; as a matter of fact, most articles using such models only study proliferation by MTS at short times (<10 days).[22,28,30] It is also known that interaction of CD44 with high molecular weight HA leads to a decreased proliferation, which is consistent with the limited increase in cell metabolism in 3D-HA constructs.

Cell morphology is dependent on culture substrate micro and macrotopography, chemistry and mechanical properties; it is well known that most cells show a fibroblastic morphology on hard and hydrophobic materials, whereas they are usually more rounded on soft hydrogels and hydrophilic materials.[47] Such differences in cell shape are not anecdotal as they influence further properties such as nucleus shape,[48] gene expression, proliferation,[49] and differentiation.[50] In the case of tumor cells, invasiveness has been shown to be related to cell morphology,[51] and spindle shape; fibroblast-like cells have been described as less aggressive than rounded cells commonly found in spheroid culture.[25] Thus, HA influence in cell shape may reflect deeper changes in the cell phenotype. To get further insights into this, phenotypic profile of cells was studied both qualitatively using immunofluorescence and quantitatively using flow cytometry. U87 is a cell line with high malignancy, showing some dedifferentiation as shown by the expression to several degrees in the different culture modes of mesenchymal marker vimentin, which in tumor cells is generally a hallmark of increased dedifferentiation and thus virulence. Nevertheless, some cells are also positive for GFAP, a marker for differentiated astrocytes, showing that a subpopulation of U87 maintains some features of differentiated cells. Generally, cells cultured in 3D culture and presence of HA tend to show increased markers of dedifferentiation such as Vimentin or Nestin. Nuclear localization of Nestin observed in 3D and 3D-HA constructs has been observed in several glioblastoma cell lines[52] as well as in U87 xenograft in an immunodeficient mouse model,[40] and is thought to contribute to the regulation of gene expression.[41] In order to investigate more quantitatively the stemness of 3D cultured U87 and the influence of HA in 3D culture, both CD133 (stemness marker) and CD44/RHAMM (HA main receptors) were studied by flow cytometry. Cytometry is currently gaining increasing acceptance for the analysis of tissue engineered constructs, as it permits a quantitative analysis of cell marker expression and study of population heterogeneity within such constructs.[27,53] CD133, or prominin, is generally described as the main CSC marker for glioma, while interaction of cells with HA through CD44 and RHAMM recruitment is known to increase malignancy.[35,36] We observed that CD44 expression was not significantly different between 2D, 3D, and 3D-HA, whereas RHAMM was upregulated in presence of HA and CD133 was upregulated in 3D and most in 3D-HA. CD44, is the main receptor of hyaluronan, and is expressed in many cancer cell types. In some cancer types, overexpression of CD44 is linked to increased malignancy of cancer cells.[54,55] Most studied is the interaction between CD44 and HA; the binding of CD44 isoforms to hyaluronan affects cell adhesion to extracellular matrix components and is implicated in the stimulation of aggregation, proliferation and migration of cancer cells. RHAMM was specifically sensible to the presence of HA in 3D culture; in glioma, RHAMM has been related to increased proliferation and migration potential, and soluble RHAMM competing with endogenous RHAMM was shown to inhibit both proliferation and migration of cells. In various cancer types, CD133+ cells have been proposed as containing a subpopulation of cancer cells with stem-like properties. CD133 positive cells have been shown to have some drug effluxing mechanisms normally found in stem cells,[56–59] which could explain their increased resistance to chemotherapy; moreover, they have DNA repair mechanisms that confer them radioresistance. Our *in vitro* experiments show that CD133 marker cell have more expression on 3D than in 2D and that presence of HA in the constructs further promotes a stem-like phenotype. The more undifferentiated phenotype observed in 3D cultures may be related with several factors, among them increased cell–cell contact in the 3D model, spatial heterogeneity, restriction in diffusion leading to central hypoxia and eventually local accumulation of acidic residues.[60] As a matter of fact, hypoxia has been described as a key factor inducing the dedifferentiation of glioma cells.[2,61] Several studies reported that porous 3D structures can significantly improve the communications of cell–ECM and provide a hypoxic microenvironment.[62,63] These intimate interactions (cell–cell and cell–substrate) provoke modifications of cell activities such as proliferation, differentiation, apoptosis, and secretion of soluble factors and deposition of ECM components, and have been shown to enhance malignant phenotypes in 3D structures; now these results tend to prove that they also increase the dedifferentiation of glioma cells and promote a CSC phenotype. RHAMM, that was significantly upregulated in presence of HA, may be implied in the crosstalk between HA microenvironment, hypoxia, and CD133 expression. Further studies with this new 3D-HA system shall shed light on the mechanisms implied.

CONCLUSIONS

In this study, we developed innovative 3D scaffolds (3D and 3D-HA) to mimic *in vitro* the structure of the tumor with controlled and tunable architectural features. Both scaffolds support cell proliferation, migration, increase of cell clustering and changes in phenotypic expression; besides, 3D-HA construct promotes overexpression of specific stem cell

surface marker CD133. This 3D-HA system leads to a natural enrichment in CSCs in standard culture conditions and may prove useful as *in vitro* model for drug development studies. Moreover, as it provides realistic cell-matrix interactions, it should permit to study the influence of microenvironment on drug and radiation resistance mechanisms by CSCs.

ACKNOWLEDGMENTS

Myriam Lebourg acknowledges CIBER-BBN for supporting her post-doc research. Cytomics Core Facility at Príncipe Felipe Research Center is thanked for the support and advice in flow cytometry experiments and Jeronimo Blanco group at ICCC for providing the U87 clone.

REFERENCES

1. Krex D, Klink B, Hartmann C, von Deimling A, Pietsch T, Simon M, Sabel M, Steinbach JP, Heese O, Reifenberger G, Weller M, Schackert G; German Glioma Network. Long-term survival with glioblastoma multiforme. Brain 2007;130:2596–2606.
2. de Almeida Sassi F, Lunardi Brunetto A, Schwartsmann G, Roesler R, Abujamra AL. Glioma revisited: From neurogenesis and cancer stem cells to the epigenetic regulation of the niche. J Oncol 2012;2012:537861.
3. Frosina G. DNA repair and resistance of gliomas to chemotherapy and radiotherapy. Mol Cancer Res 2009;7:989–999.
4. Venere M, Fine HA, Dirks PB, Rich JN. Cancer stem cells in gliomas: Identifying and understanding the apex cell in cancer's hierarchy. Glia 2011;59:1148–1154.
5. Germano I, Swiss V, Casaccia P. Primary brain tumors, neural stem cell, and brain tumor cancer cells: Where is the link? Neuropharmacology 2010;58:903–910.
6. Yoon CH, Hyun KH, Kim RK, Lee H, Lim EJ, Chung HY, An S, Park MJ, Suh Y, Kim MJ, Lee SJ. The small GTPase Rac1 is involved in the maintenance of stemness and malignancies in glioma stem-like cells. FEBS Lett 2011;585:2331–2338.
7. Cheng JX, Liu BL, Zhang X. How powerful is CD133 as a cancer stem cell marker in brain tumors? Cancer Treat Rev 2009;35: 403–408.
8. Filatova A, Acker T, Garvalov BK. The cancer stem cell niche(s): The crosstalk between glioma stem cells and their microenvironment. Biochim Biophys Acta 2013;1830:2496–2508.
9. deCarvalho AC, Nelson K, Lemke N, Lehman NL, Arbab AS, Kalkanis S, Mikkelsen T. Gliosarcoma stem cells undergo glial and mesenchymal differentiation in vivo. Stem Cells 2010;28: 181–190.
10. Qiu B, Zhang D, Tao J, Wu A, Wang Y. A simplified and modified procedure to culture brain glioma stem cells from clinical specimens. Oncol Lett 2012;3:50–54.
11. Yu SC, Ping YF, Yi L, Zhou ZH, Chen JH, Yao XH, Gao L, Wang JM, Bian XW. Isolation and characterization of cancer stem cells from a human glioblastoma cell line U87. Cancer Lett 2008;265: 124–134.
12. Abbott A. Cell culture: Biology's new dimension. Nature 2003;424: 870–872.
13. Cukierman E, Pankov R, Stevens DR, Yamada KM. Taking cell-matrix adhesions to the third dimension. Science 2001;294: 1708–1712.
14. Hsiao AY, Torisawa YS, Tung YC, Sud S, Taichman RS, Pienta KJ, Takayama S. Microfluidic system for formation of PC-3 prostate cancer co-culture spheroids. Biomaterials 2009;30:3020–3027.
15. Kim JB. Three-dimensional tissue culture models in cancer biology. Semin Cancer Biol 2005;15:365–377.
16. Sonoda T, Kobayashi H, Kaku T, Hirakawa T, Nakano H. Expression of angiogenesis factors in monolayer culture, multicellular spheroid and in vivo transplanted tumor by human ovarian cancer cell lines. Cancer Lett 2003;196:229–237.
17. Hirschhaeuser F, Menne H, Dittfeld C, West J, Mueller-Klieser W,Kunz-Schughart LA. Multicellular tumor spheroids: An underestimated tool is catching up again. J Biotechnol 2010;148:3–15.
18. Debnath J, Brugge JS. Modelling glandular epithelial cancers in three-dimensional cultures. Nat Rev Cancer 2005;5:675–688.
19. Debnath J, Muthuswamy SK, Brugge JS. Morphogenesis and oncogenesis of MCF-10A mammary epithelial acini grown in three-dimensional basement membrane cultures. Methods 2003; 30:256–268.
20. Lee GY, Kenny PA, Lee EH, Bissell MJ. Three-dimensional culture models of normal and malignant breast epithelial cells. Nat Methods 2007;4:359–365.
21. Pampaloni F, Reynaud EG, Stelzer EH. The third dimension bridges the gap between cell culture and live tissue. Nat Rev Mol Cell Biol 2007;8:839–845.
22. Horning JL, Sahoo SK, Vijayaraghavalu S, Dimitrijevic S, Vasir JK, Jain TK, Panda AK, Labhasetwar V. 3-D tumor model for in vitro evaluation of anticancer drugs. Mol Pharm 2008;5:849–862.
23. Kang SW, Bae YH. Cryopreservable and tumorigenic three-dimensional tumor culture in porous poly(lactic-co-glycolic acid) microsphere. Biomaterials 2009;30:4227–4232.
24. Dhiman HK, Ray AR, Panda AK. Three-dimensional chitosan scaffold-based MCF-7 cell culture for the determination of the cytotoxicity of tamoxifen. Biomaterials 2005;26:979–986.
25. Kievit FM, Florczyk SJ, Leung MC, Veiseh O, Park JO, Disis ML, Zhang M. Chitosan-alginate 3D scaffolds as a mimic of the glioma tumor microenvironment. Biomaterials 2010;31:5903–5910.
26. Leung M, Kievit FM, Florczyk SJ, Veiseh O, Wu J, Park JO, Zhang M. Chitosan-alginate scaffold culture system for hepatocellular carcinoma increases malignancy and drug resistance. Pharm Res 2010;27:1939–1948.
27. Chen L, Xiao Z, Meng Y, Zhao Y, Han J, Su G, Chen B, Dai J. The enhancement of cancer stem cell properties of MCF-7 cells in 3D collagen scaffolds for modeling of cancer and anti-cancer drugs. Biomaterials 2012;33:1437–1444.
28. Gurski LA, Jha AK, Zhang C, Jia X, Farach-Carson MC. Hyaluronic acid-based hydrogels as 3D matrices for in vitro evaluation of chemotherapeutic drugs using poorly adherent prostate cancer cells. Biomaterials 2009;30:6076–6085.
29. Hutmacher DW. Biomaterials offer cancer research the third dimension. Nat Mater 2010;9:90–93.
30. Fischbach C, Chen R, Matsumoto T, Schmelzle T, Brugge JS, Polverini PJ, Mooney DJ. Engineering tumors with 3D scaffolds. Nat Methods 2007;4:855–860.
31. Loessner D, Stok KS, Lutolf MP, Hutmacher DW, Clements JA, Rizzi SC. Bioengineered 3D platform to explore cell-ECM interactions and drug resistance of epithelial ovarian cancer cells. Biomaterials 2010;31:8494–8506.
32. Stern R. Hyaluronan metabolism: A major paradox in cancer biology. Pathol Biol (Paris) 2005;53:372–382.
33. Auvinen P, Tammi R, Kosma VM, Sironen R, Soini Y, Mannermaa A, Tumelius R,Uljas E, Tammi M. Increased hyaluronan content and stromal cell CD44 associate with HER2 positivity and poor prognosis in human breast cancer. Int J Cancer 2013;132:531–539.
34. Tamada Y, Takeuchi H, Suzuki N, Aoki D, Irimura T. Cell surface expression of hyaluronan on human ovarian cancer cells inversely correlates with their adhesion to peritoneal mesothelial cells. Tumour Biol 2012;33:1215–1222.
35. Toole BP. Hyaluronan promotes the malignant phenotype. Glycobiology 2002;12:37R–42R.
36. Ward JA, Huang L, Guo H, Ghatak S, Toole BP. Perturbation of hyaluronan interactions inhibits malignant properties of glioma cells. Am J Pathol 2003;162:1403–149.
37. Lebourg M, Suay Anton J, Gomez Ribelles JL. Hybrid structure in PCL-HAp scaffold resulting from biomimetic apatite growth. J Mater Sci Mater Med 2010;21:33–44.
38. Darr A, Calabro A. Synthesis and characterization of tyramine-based hyaluronan hydrogels. J Mater Sci Mater Med 2009;20:33–44.
39. Chen J, Wang J, Chen D, Yang J, Yang C, Zhang Y, Zhang H, Dou J. Evaluation of characteristics of CD44+CD117+ ovarian cancer stem cells in three dimensional basement membrane extract scaffold versus two dimensional monocultures. BMC Cell Biol 2013;14:7.
40. Strojnik T, Kavalar R, Lah TT. Experimental model and immunohistochemical analyses of U87 human glioblastoma cell

xenografts in immunosuppressed rat brains. Anticancer Res 2006; 26:2887–2900.
41. Krupkova O Jr, Loja T, Redova M, Neradil J, Zitterbart K, Sterba J, Veselska R. Analysis of nuclear nestin localization in cell lines derived from neurogenic tumors. Tumour Biol 2011;32:631–639.
42. Fischbach C, Kong HJ, Hsiong SX, Evangelista MB, Yuen W, Mooney DJ. Cancer cell angiogenic capability is regulated by 3D culture and integrin engagement. Proc Natl Acad Sci USA 2009; 106:399–404.
43. Lebourg M, Rochina JR, Sousa T, Mano J, Ribelles JL. Different hyaluronic acid morphology modulates primary articular chondrocyte behavior in hyaluronic acid-coated polycaprolactone scaffolds. J Biomed Mater Res A 2013;101:518–527.
44. Ródenas-Rochina J, Ribelles JL, Lebourg M. Comparative study of PCL-HAp and PCL-bioglass composite scaffolds for bone tissue engineering. J Mater Sci Mater Med 2013;24:1293–1308.
45. Ng KW, Leong DT, Hutmacher DW. The challenge to measure cell proliferation in two and three dimensions. Tissue Eng 2005;11: 182–191.
46. Huyck L, Ampe C, Van Troys M. The XTT cell proliferation assay applied to cell layers embedded in three-dimensional matrix. Assay Drug Dev Technol 2012;10:382–392.
47. Mason, Brooke N. Matrix stiffness: A regulator of cellular behavior and tissue formation. In: Bhatia SK, editor. Engineering Biomaterials for Regenerative Medicine: Novel Technologies for Clinical Applications. Springer; 2012.
48. Lovett DB, Shekhar N, Nickerson JA, Roux KJ, Lele TP. Modulation of nuclear shape by substrate rigidity. Cell Mol Bioeng 2013; 6:230–238.
49. Mammoto A, Ingber DE. Cytoskeletal control of growth and cell fate switching. Curr Opin Cell Biol 2009;21:864–870.
50. McBeath R, Pirone DM, Nelson CM, Bhadriraju K, Chen CS. Cell shape, cytoskeletal tension, and RhoA regulate stem cell lineage commitment. Dev Cell 2004;6:483–495.
51. Yamaguchi H, Wyckoff J, Condeelis J. Cell migration in tumors. Curr Opin Cell Biol 2005;17:559–564.
52. Doan LL, Tanner MK, Grimes HL. Intranuclear staining of proteins in heterogeneous cell populations and verification of nuclear localization by flow cytometric analysis. J Immunol Methods 2003;279:193–198.
53. Huang J, Zhang H, Yu Y, Chen Y, Wang D, Zhang G, Zhou G, Liu J, Sun Z, Sun D, Lu Y, Zhong Y. Biodegradable self-assembled nanoparticles of poly(D,L-lactide-*co*-glycolide)/hyaluronic acid block copolymers for target delivery of docetaxel to breast cancer. Biomaterials 2014;35:550–566.
54. Koochekpour S, Pilkington GJ, Merzak A. Hyaluronic acid/CD44H interaction induces cell detachment and stimulates migration and invasion of human glioma cells in vitro. Int J Cancer 1995;63: 450–454.
55. Turley EA, Noble PW, Bourguignon LY. Signaling properties of hyaluronan receptors. J Biol Chem 2002;277:4589–4592.
56. Hirschmann-Jax C, Foster AE, Wulf GG, Goodell MA, Brenner MK. A distinct "side population" of cells with high drug efflux capacity in human tumor cells. Proc Natl Acad Sci USA 2004;101: 14228–14233.
57. Hirschmann-Jax C, Foster AE, Wulf GG, Goodell MA, Brenner MK. A distinct "side population" of cells in human tumor cells: Implications for tumor biology and therapy. Cell Cycle 2005;4:203–205.
58. Liu G, Yuan X, Zeng Z, Tunici P, Ng H, Abdulkadir IR, Lu L, Irvin D, Black KL, Yu JS. Analysis of gene expression and chemoresistance of CD133+ cancer stem cells in glioblastoma. Mol Cancer 2006;5:67.
59. Bleau AM, Hambardzumyan D, Ozawa T, Fomchenko EI, Huse JT, Brennan CW, Holland EC. PTEN/PI3K/Akt pathway regulates the side population phenotype and ABCG2 activity in glioma tumor stem-like cells. Cell Stem Cell 2009;4:226–235.
60. Hjelmeland AB, Wu Q, Heddleston JM, Choudhary GS, MacSwords J, Lathia JD, McLendon R, Lindner D, Sloan A, Rich JN. Acidic stress promotes a glioma stem cell phenotype. Cell Death Differ 2011;18:829–840.
61. Soeda A, Park M, Lee D, Mintz A, Androutsellis-Theotokis A, McKay RD, Engh J, Iwama T, Kunisada T, Kassam AB, Pollack IF, Park DM. Hypoxia promotes expansion of the CD133-positive glioma stem cells through activation of HIF-1alpha. Oncogene 2009; 28:3949–3959.
62. Ong SM, Zhao Z, Arooz T, Zhao D, Zhang S, Du T, Wasser M, van Noort D, Yu H. Engineering a scaffold-free 3D tumor model for in vitro drug penetration studies. Biomaterials 2010;31:1180–1190.
63. Ruan K, Song G, Ouyang G. Role of hypoxia in the hallmarks of human cancer. J Cell Biochem 2009;107:1053–1062.